EFFECT OF ANNEALING ON THE SECONDARY PARTICLES EMISSION FROM THE ZIRCONIUM ALLOY SURFACE

I.A. Afanasieva[1], V.V. Bobkov[1], V.V. Gritsyna[1], K.V. Kovtun[2], V.T. Koppe[1], V.A. Litvinov[1], I.I. Okseniuk[1], S.V. Hovrich [2], D.I Shevchenko[1]

[1]V.N. Karazin Kharkiv National University, Kharkov, Ukraine;

[2]National Science Center "Kharkov Institute of Physics and Technology", Kharkov, Ukraine

The emission of secondary ions and excited particles under ion bombardment of the zirconium alloy (metallic glass) was studied by methods of secondary ion mass spectrometry (SIMS) and ion-photon spectrometry (IPS). It was ascertained that the dependence of the secondary particles yield on the radiation dose (up to $3.5 \cdot 10^{17}$ ion·cm^{-2}) is different for the particles knocked out from the chemical compounds surface and for those knocked out from the target volume. It is shown that the spatial distribution of the secondary excited particles the amorphous metallic glass differs from that for the crystalline glass. From the analysis of the effect of resonant ionization process on the probability flying off of the excited particles, the work function of the bulk metallic glasses $Zr_{41}Ti_{14}Cu_{12.5}Ni_{10}Be_{22.5}$ ($3.93 < \varphi < 4.131$ eV) was estimated.

PACS: 34.50.Gb; 34.50.Fa; 32.30.Jc; 71.20.Ps; 79.20.Rf –

INTRODUCTION

Class of metallic solids with amorphous structure, which is characterized by lack of long-range order in the atomic arrangement, is called bulk metallic glass (BMG). Usually BMG are much stronger than their crystalline analogs since the amorphous structure has no defects and internal stresses typical for the lattice which can reduce the material resistance to loads of various kinds. However, BMG have a serious drawback – they are sensitive to heat, i. e., the temperature rise causes active crystal formation [1] which may result in the structure heterogeneity. In this regard, it is very important to develop methods allowing to detect the start of the crystal formation process in BMG, which particularly happens while their heating.

At ion bombardment of the solid surfaces by beams of accelerated ions a number of physical phenomena and processes occur. They are: the reflection of the some part of bombarding ions, secondary ion emission (SIE), the excited particle emission with the subsequent emission of photons (ion-photon emission – IPE), Auger electron emission, ion-electron potential and kinetic emission, etc [2]. Now some of these phenomena have formed the basis of various methods for surface diagnostics allowing qualitative and quantitative analysis of the surface elemental composition, observing the processes of oxidation and catalysis on the surface, determining the volume distribution of impurities in solid targets, analyzing the extent of the surface modification caused by ion irradiation, etc. Among many diagnostic techniques the methods of surface study based on SIE and IPE phenomena – methods of secondary ion mass spectrometry (SIMS) and ion-photon spectrometry (IPS) should be emphasized. SIMS, as a direct method of determining elemental, isotopic, or molecular composition of any solids and many liquids of inorganic and organic origin, allows to obtain data on the elemental composition, distribution of elements in depth (profiling) as well as on physical-chemical processes occurring on the sample surface. Here, the high sensitivity of this method, which provides the impurity atoms concentration of $\sim 10^{12}\ldots10^{16}$ cm^{-3} ($\sim 10^{-4}\ldots10^{-7}$%), and substance consumption of $\sim 10^{-14}\ldots10^{-15}$ g (which makes $\sim 10^{-6}$ of monatomic layer) should be noted. IPS, in its turn, allows not only obtaining information about the nature of flying off particles and their kinetic energy, but also determining the particles on their excited states what allows to obtain data on the elemental composition of the studied material and to draw conclusions about the processes that lead to fly off the particles in the excited state [3–5]. The undoubted advantage of IPS method is a relative simplicity of the experimental equipment required to its implementation.

To research the heat effect on modification of the composition and properties of surface of amorphous metal alloys, the bulk metallic glasses $Zr_{41}Ti_{14}Cu_{12.5}Ni_{10}Be_{22.5}$ produced by vacuum arc melting, and subjected to annealing at different temperatures, were studied by SIMS and IPS methods.

EXPERIMENTAL TECHNIQUE

In the process of zirconium alloy $Zr_{41}Ti_{14}Cu_{12.5}Ni_{10}Be_{22.5}$ research by SIMS method the monolithic samples of the alloy were irradiated by Ar^+ ion beam with energy of 8 keV. The residual vacuum in the target chamber was $4 \cdot 10^{-4}$ Pa, the current density of the primary beam was 1.5…6.0 μA·cm^{-2}, what corresponds to the dynamic SIMS mode. The system of secondary ion analysis had a double focusing: by mass and energy. The secondary ion beam formed by the lens system was directed into the segment magnetic analyzer, in which ions were separated by ratio m/e, and then the secondary ions got into the energy analyzer of a cylindrical deflector type serving as an energy filter. The secondary ion recording system allowed recording particles with energy $E \sim 15$ eV and energy spread ΔE of ~ 10 eV. Measurement of emission intensity of secondary ions was carried out within the dynamic range making at least 6 orders of magnitude.

IPS studies were conducted on an experimental device to obtain mass selected beam of Ar^+ ions with energy of 20 keV and current density of 15 μkA·cm^{-2} ($P_{res} \sim 5 \cdot 10^{-4}$ Pa) [6]. The target location relative to the

photoelectric recording system allowed separating the emission of the flying off excited particles from the probably ion luminescence of the target surface. The angle between the direction of the beam incident on the target surface and the normal to the surface was 45°. The radiation in the range 250…800 nm emitted by the excited sputtered particles was analyzed with monochromator MDR-3 (Optical Mechanical Association, St Petersburg) and registered using a cooled photomultiplier FEU-106 (Electro-Lamp Plant, Moscow) by photon counting.

The bulk metallic glasses $Zr_{41}Ti_{14}Cu_{12.5}Ni_{10}Be_{22.5}$ investigated in the paper, were produced by the method of electric-arc vacuum melting in a non-consumable electrode device. For melting the samples, high pure initial components containing not less than 99.9 wt.% of the base metal was used. Zirconium and titanium, by iodide cleaning, nickel cathode, electrical copper, and distilled beryllium were used as initial materials. To obtain a homogeneous composition of the fused material, multiple remelting of the ingot with its 180° turning in the ingot mold was used. Thus a sample of the bulk metallic glass $Zr_{41}Ti_{14}Cu_{12.5}Ni_{10}Be_{22.5}$ with a diameter of 25…28 mm, thickness of 10…14 mm and weight of about 25 grams was obtained. The further step in preparation of the sample for the analysis was the choice of annealing temperature at which the melted amorphous alloy would form a crystal structure. According to [7], where the process of crystal phases formation similar in composition to the alloy ($Zr_{50}Ti_{16}Cu_{15}Ni_{19}$) was studied, the temperatures ~ 725 and 773 K defined the onset of the second stage crystallization and its completion, respectively. Therefore, from the ingot obtained in the course of melting by electric erosion machining some objects to be studied were cut for preparation of three samples: sample 1 – initial, sample 2 – annealed at temperature of 723 K, sample 3 – annealed at temperature of 773 K. The samples of the bulk metallic glass were annealed in a vacuum furnace for 1 hour.

The annealed samples of zirconium alloy $Zr_{41}Ti_{14}Cu_{12.5}Ni_{10}Be_{22.5}$ were tested for the presence of crystalline phase using an X-ray diffractometer DRON-4-07. Here, Bragg-Brentano X-ray optics with double Soller slit was used. Recording was conducted with a proportional counter, for CuK_α radiation filtered from K_β radiation. The tube voltage was 37 V, current – 16 A. The angular resolution was about 0.085° (on 2θ); angular inaccuracy – not more than 0.02°. Time constant in the angular form was as follows: at the normal view – about 0.008°, at the plain view – 0.08°. The survey was done with computer check-points – from 10 to 50 pixels per degree. The angular position offset for each point by half the angular step was taken into account.

Fig. 1 shows the results of X-ray diffraction obtained for the three types of samples. It turned out that for samples 1 and 2 the dependence plot of relative intensity of X-ray reflections from the sample angle showed a diffuse hump typical of the amorphous structure. Annealing at T = 773 K for 1 hour alters significantly the results of X-ray diffraction. The diffuse scattering maximum covering the corners ~ 30…50°. In its place, in the sample annealed at T = 773 K, sharp peaks characteristic of crystalline structure are recorded. Analysis of the obtained diffraction pattern allows making a conclusion that after this heat treatment in sample 3 crystalline phases are present. Thus, the annealing at T = 773 K leads to ordering of atoms in the alloy $Zr_{41}Ti_{14}Cu_{12.5}Ni_{10}Be_{22.5}$.

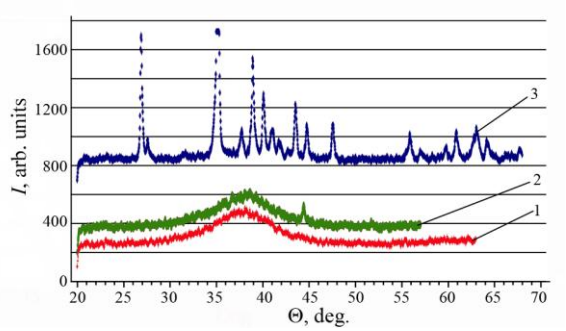

Fig. 1. Results of x-ray diffraction obtained on the initial sample (1); annealed at the temperature of 723 K (2); annealed at temperature of 773 K (3)

EXPERIMENTAL RESULTS AND ISCUSSION

STUDY BY SIMS METHOD

Method of secondary ion mass spectrometry (SIMS) was used for studying samples of zirconium alloy $Zr_{41}Ti_{14}Cu_{12.5}Ni_{10}Be_{22.5}$. Mass spectra of low-energy positive secondary ions sputtered from the surfaces were measured for the samples: initial (sample 1); annealed at 723 K (sample 2); annealed at 773 K (sample 3). The primary ions are Ar^+ with energy of 8 keV, current density of 3.0 μA·cm^{-2}, residual vacuum in the chamber target of (2…3)·10^{-5} Pa.

The dependence of emission intensity for different secondary ions on the radiation dose (by primary ions) were investigated in the range of 0…3.5·10^{17} ion·cm^{-2}.

The measurements showed these mass spectra are characteristic for metallic samples in these experimental conditions. The following emissions are typical for the mass spectra:

matrix secondary ions (corresponding to each alloy component);

secondary ions of oxides;

secondary ions of hydrides and hydroxides;

secondary ions of carbides;

cluster secondary ions of the alloy components (and their compounds with hydrogen, oxygen);

complex secondary ions including different alloy components;

secondary ions of hydrogen, carbon, oxygen, hydrocarbons (and their fragments), caused by fragmentation of surface chemical compounds both present initially on the surface, and resulting from the current interaction with the gas phase.

The richest spectrum of secondary ions for zirconium is Zr^+, ZrH^+, ZrO^+, ZrO_2^+, $ZrOH^+$, ZrO_2H^+, ZrC^+, ZrC_2^+, $ZrCH^+$, ZrC_2H^+, ZrC_2OH^+, $ZrTi^+$, $ZrTiO^+$,$ZrTiO_2^+$, Zr_2^+, Zr_2O^+, $Zr_2O_2^+$, $Zr_2O_3^+$.

As an example, Fig. 2 shows mass spectrum sections of the secondary ions sputtered from the surface of the initial sample at the initial radiation dose.

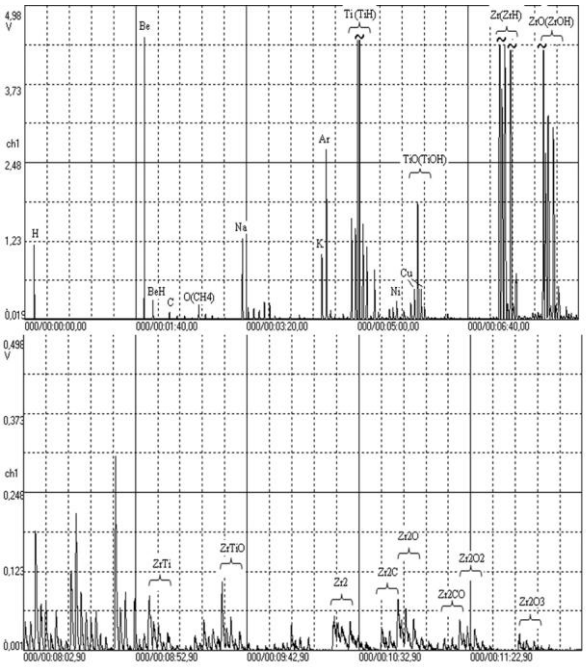

Fig. 2. Sections of the mass spectrum of low-energy positive secondary ions sputtered from the surface of the initial sample (for convenience multi-grams are given with the difference in sensitivity of one order)

It is difficult to determine the amount of certain compounds on the surface basing on the emission intensity as here is no information about coefficients of secondary ion emission from these compounds, besides, one should take into account the matrix effect, etc. To obtain the quantitative information some special complex and time-consuming researches are required. Therefore, all the information given below is only qualitative.

Further we give the dependence of intensity (in relative units) of the secondary ion emission on the irradiation dose (Figs. 3–5). As long as most of the alloy components are not monoisotopic, the information is provided for the most common isotopes or those free from superposition; the percentage recalculation for 100 % was not made.

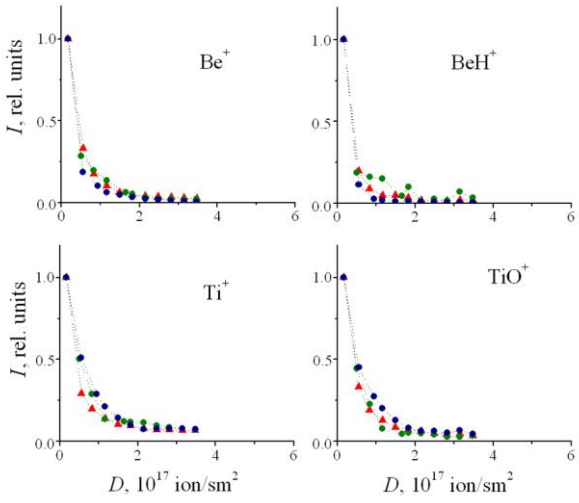

Fig. 3. Dose dependences of ions Be^+, BeH^+, Ti^+ and TiO^+: ▲ – sample 1; ● – sample 2; ● – sample 3

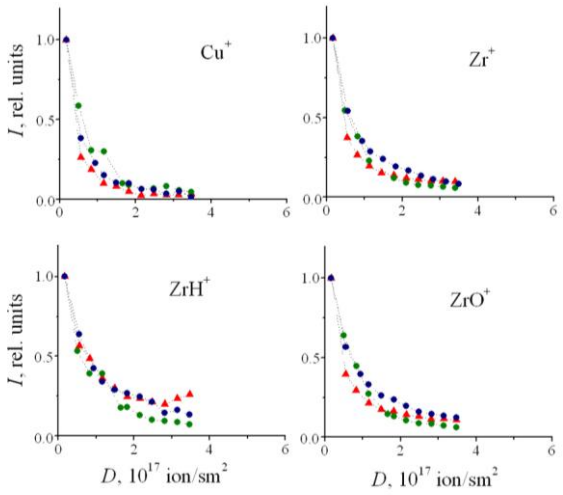

Fig.4. Dose dependence of the ions Cu^+, Zr^+, ZrH^+ and ZO^+: ▲ – sample 1; ● – sample 2; ● – sample 3

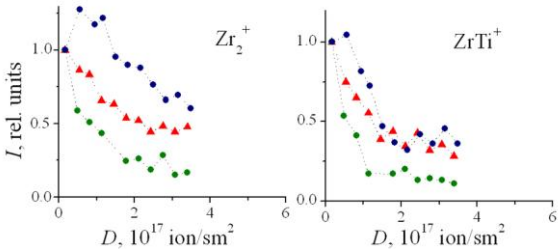

Fig.5. Dose dependence of ions Zr_2^+, ZrTi: ▲ – sample 1; ● – sample 2; ● – sample 3

Figs. 3–5 show three types of dose dependences: a sharp decrease in the intensity of the ion yield at the beginning of the ion bombardment followed by a slight decline in the course of the following bombardment (see Fig. 3), a fairly uniform drop in intensity (see Fig. 5), and the intermediate type of dependence (see Fig.4). In [8] it is noted that this difference in dose dependencies of the sputtered secondary particles is determined by some different processes causing their knocking-out. In the first case these are particles knocked out of the surface compounds whose number rapidly decreases under ion bombardment due to the surface purification. In the second case these are ions knocked out of the target volume. Finally, in the third case it is a superposition of the first two cases. It should be noted that for all three types of targets (initial, and annealed at temperatures 723 and 773 K) there is no significant change in the yield of ions of the type MeO^+ and MeH^+ knocked out of the target volume. It shows that at these temperatures there is no significant desorption of hydrogen and oxygen from the target volume. In [9] it has been noted that hydrogen release in the system of quick-hardened Ti-Zr-Ni alloys occurs within the temperature range of 500…700º C with its maximum at 600º C. Similar statement is likely to be true for oxygen as well.

Analysis of the obtained results allows drawing the following conclusions.

In the mass spectra of all three samples the same emissions occur, i.e., annealing at both 723 and 773 K did not result in forming any additional chemical compounds on the sample surface.

The difference between the studied samples is in the fact that the intensity of almost all emissions for sample 3 (annealed at 773 K) is higher then those for samples 1 and 2. This is especially true for beryllium. For samples 1 and 2 the intensity of the respective emissions, is practically the same. However, it does not mean that for different secondary ions the variation of the dose dependencies is the same.

As the radiation dose increases the intensity of emission of all the observed secondary ions decreases. This shows, first of all, that the overwhelming majority of secondary ions are sputtered from the chemical compounds on the surface (since it is the low-energy component of the secondary ions that is recorded). And, then, the number of these chemical compounds on the surface decreases, i.e., the surface area covered by these compounds decreases, stoichiometric ratio of the compounds changes, and the surface depurates. This behavior is typical for all three samples (as well as for many metal targets). It should be noted that the dependence of the secondary ion intensity on the irradiation dose is the same almost for all emissions. The exceptions are the cluster ions Zr_2^+ and $ZrTi^+$, as well as H^+, whose intensity with increase of the irradiation dose decreases much less, and Be^+ and BeH^+, whose intensity with increase of the irradiation dose decreases much more. In respect of the cluster ions one may suppose that they are knocked out not only of the complex compounds on the target surface, but also of the target volume. In [10] it is noted that when bombarding metals by heavy ions a large number of cluster ions, whose maximum energy distribution is in the region of several eV, are knocked out. So, they, just like ions knocked out of the compounds on the surface, belong to the low-energy component of the secondary ions for whose registration the device system is tuned up.

With high irradiation doses the intensity of secondary ion emission tends to reach the plateau. The spectra become much purer. In this case, the secondary ions are sputtered both from the "pure" surface (free from nitrogen compounds), and from the compounds formed on the surface in dynamic mode due to interaction with the residual gas phase (oxygen, hydrogen, hydrocarbons), as well as from the compounds that may be present in the samples volume. The degree of the surface covering by compounds due to the interaction with the gas phase is determined by the dynamic equilibrium between the processes of chemical bonds formation and that of the process of sputtering by the primary beam.

STUDY BY IPS METHOD

IPS method was used to study samples of zirconium alloy (initial and annealed at temperature of 723 and 773 K). The samples were bombarded by Ar^+ ions with the energy of 20 keV and current density of 15 $\mu A \cdot cm^{-2}$. The residual vacuum in the target chamber was $5 \cdot 10^{-4}$ Pa. Emission spectra of the knocked out excited particles were studied in the wavelength region of 250.0…800.0 nm.

Analysis of the obtained spectra showed that intrinsically observed lines are the following:

λλ 332.1 nm Be I, 313.0 nm Be II;
λλ 521.0 nm, 519.2 nm, 517.3 nm Ti I;
λλ 327.3 nm, 324.7 nm Cu I;
λλ 457.5 nm, 468.7 nm Zr I.

It should be noted that the intensity of Ni I spectral lines is low. This causes a considerable error in the analysis results. Therefore, the paper does not describe the results related to the emission of nickel particles.

The dependences of the quantum yield of the excited particle emission on the irradiation dose of the sample by the primary beam of Ar^+ in the dose range from 0 to $6 \cdot 10^{17}$ ion·cm^{-2} were obtained for each of these lines. The values of the radiation quantum yield are in the range of $(30…200) \cdot 10^{-6}$ photons per one incident ion for a time unit, and do not change considerably in the course of the ion bombardment. For easy comparison of IPS and SIMS data the dose dependences of spectral lines intensity and of mass spectra are compared in relative units.

Figs. 6 and 7 show the dose dependences of the radiation intensity of the above lines for the tested samples.

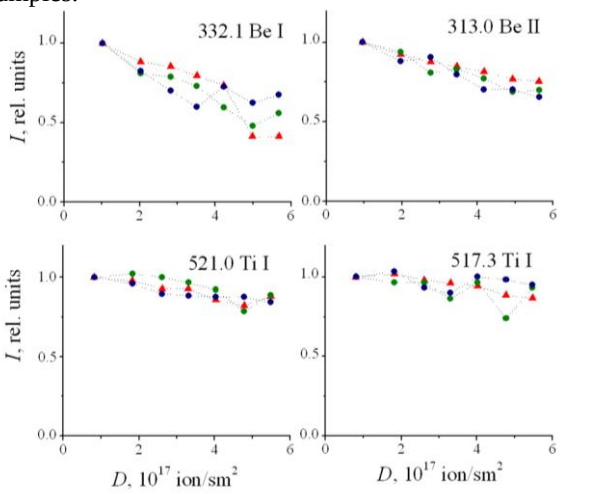

Fig. 6. Dose dependences of the intensity (in relative units) of lines λ332.1 nm Be I; λ313.0 nm Be II; λ521.0 nm Ti I u λ517.3 nm Ti I: ▲ – sample 1; ● – sample 2; ● – sample 3

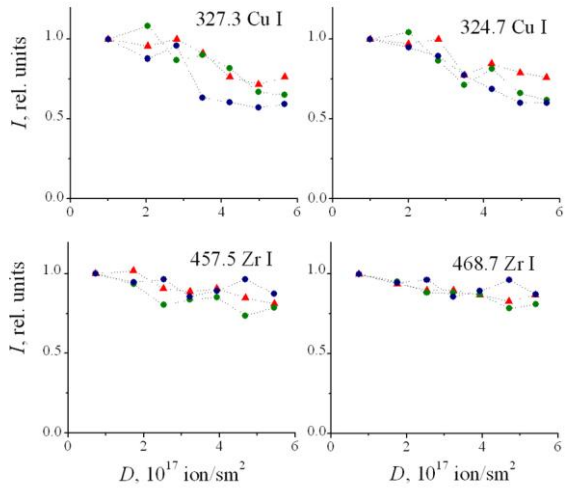

Fig. 7. Dose dependences of the intensity (in relative units) of lines λ327.3 nm Cu I; λ324.7 nm Cu I; λ457.5 nm Zr I and λ468.7 nm Zr I: ▲ – sample 1; ● – sample 2; ● – sample 3

One can see that the dose dependence variations of the intensities of the spectral lines emitted by knocked out excited atoms and ions of the elements –components of the alloy, first, are similar both for different elements and for different targets; second, are similar to the dose variation for the cluster ions shown in Fig. 5.

The next step was to study the spatial distribution of radiation of the knocked out excited particles to determine their kinetic energy. It is known [11] that the intensity dependence of spectral line (I) on distance (l) from the target surface can be expressed by the formula:

$$I = const \cdot \exp(-l/(\upsilon_{eff} \cdot \tau)), \qquad (1)$$

where υ_{eff} is the effective velocity of the group of knocked out particles, τ is the lifetime of the excited state. In spite of the difficulty to determine physical meaning of the term "effective speed", its value is used to determine the type of the process that leads to knocking out of a certain group of particles. They can be slow particles, formed by the development of the collision cascade in a solid in the process of ion bombardment, as well as fast particles formed in the process of multiple collisions of an incident ion with particles of the target surface [12]. In the first case the energy of such particles is several tens of eV (if the collision cascade is developed from the depth of the target volume), and several hundreds of eV (when the collision cascade is developed near the surface). The kinetic energy of the particles formed in the process of multiple collisions is comparable with the energy of the primary beam. As it follows from formula (1), basing on the experimentally obtained dependence ln $I(l)$ one can determine the value of the effective velocity of a group of particles (their kinetic energy), and draw conclusions about the process of their knocking out. The dependences ln $I(l)$ were obtained using a special nozzle on the spectrograph entrance slit, which allows moving a 0.1 mm wide horizontal slit along the image of the luminous region over the target surface in the plane of the spectrograph entrance slit. Correlation of the plots of ln $I(l)$ dependence for the emissions on two targets, the initial, and the annealed at temperature of 773 K, is presented in Fig. 8.

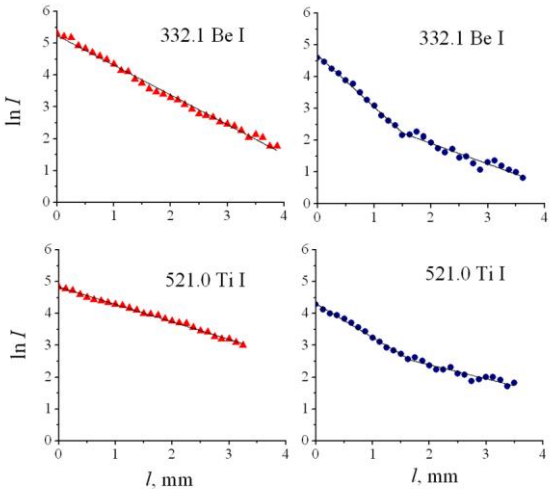

Fig. 8. Spatial distribution of emission of the knocked out excited particles ▲ – sample 1; ● – sample 3

The difference between these plots is evident from the first sight. For the initial (unannealed) samples the experimental points fall on one straight line, by whose slope angle tangent the values of the kinetic energy of flying off excited particles, emitting photons with wavelength shown on the plot, can be estimated. For the samples annealed at temperature of 773 K the experimental points can be approximated by two straight lines with different slopes. Therefore, the contribution to the studied radiation spatial distribution is made by particles of two velocity groups. The table gives kinetic energy values defined for these groups of particles. Also, the table gives the wavelength for the emissions under study, their interpretation, electron transition and the value of electron affinity μ (the distance between the excited level under study and the vacuum level).

Values of kinetic energy of sputtered excited particles

λ, nm	Interpretation	Transition	μ, eV	Kinetic energy, eV		
				Initial	Annealed at 773 K	
332.1	Be I	$3s\ ^3S \rightarrow 2p\ ^3P^o$	2.87	2200	430	14000
313.0	Be II	$2p\ ^2P^o \rightarrow 2s\ ^2S$	14.22	900	200	1500
521.0	Ti I	$z\ ^3F^o \rightarrow a\ ^3F$	4.39	42	3	64
327.3	Cu I	$4p\ ^2P^o_{1/2} \rightarrow 4s\ ^2S_{1/2}$	3.94	9000	1260	13000
457.5	Zr I	$z\ ^3G^o \rightarrow a\ ^3F$	4.13	120	22	420
468.7	Zr I	$y\ ^5G^o \rightarrow a\ ^5F$	3.47	1400	1500	20000

It is evident that in the case with annealed sample, which is characterized by crystal structure, the contribution is made by relatively slow particles, due to the collision cascade in the volume of the tested target. In the case with the initial sample with amorphous structure the collision cascade in the sample volume is less probable.

Fig. 9 presents the arrangement of the energy levels for the examined excited states relative to the vacuum level and suggests Fermi level position (the value of the work function) of the alloy obtained from the analysis of the velocity set for the flying off excited particles with the influence of nonradiative loss process of excitation of the resonant ionization (RI) taken into account.

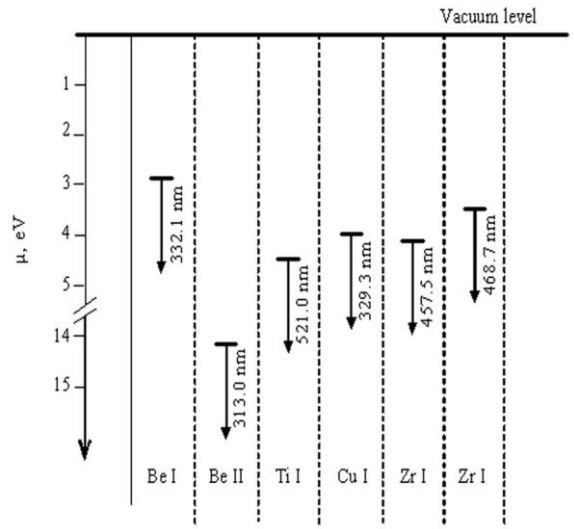

Fig. 9. Arrangement of the energy levels for the excited states of flying off particles relative to the vacuum level

It is known that for any process of formation of particles knocked out of a solid at the ion bombardment [13], the final formation of the excited state of the flying off particle is influenced by nonradiative loss excitation of Auger and resonant type. In this case, the probably occurrence of these processes is inversely proportional to the velocity of the flying off particle. In particular, if the electron transition of the flying off particle from the level of the excited state to a free (vacant) level of the electron structure of a solid is possible, then, due to such a transition, the flying off particle looses its excitation. From the analysis of the results given in the table and in Fig. 9, it is evident, that for lines λ521.0 nm Ti I and λ457.5 nm Zr I the contribution of slow particles emission is observed for both types of the target. This allows assuming that the energy levels of the excited state, whose decay causes the emission of these lines, are resonant to the filled region of the conductivity band of the alloy. The electron resonant transmission from the excited state to the conductivity band is impossible, what results in spontaneous decay of the excited state accompanied by photon emission. On the rest of atomic lines for the both targets only fast particle emission is observed. The levels of the appropriate excited states are apparently resonant to the free (not occupied by electrons) conductivity band. In this case, the loss of excitation is possible due to the process of resonant ionization (RI). In [13] it is shown that for the flying off particle the probability to preserve the excitation (P), avoiding RI process is determined by the formula:

$$P = \exp[-(A/a)\cdot \upsilon^{-1}], \qquad (2)$$

where (A/a) are RI process constants, υ is the velocity of the flying off excited particle. Hence, only the fastest particles preserve the excitation when flying off from the surface which is followed by spontaneous photon emission. It allows to suggest that the value of the work function (φ) of the studied alloy is in the range of $3.93 < \varphi < 4.131$ eV. Such a value of the examined zirconium alloy work function is close to the value of the work function of the similar alloy, described in [14].

As to ion line λ313.0 nm Be II the following should be noted: for the excited state, whose decay results in this line emission, the effect of RI process is highly improbable, but in papers [15, 16] it is noted that the ions excitation may be formed as the result of hard collisions of the primary ion and a particle in the target, at which the particle gains a considerable kinetic energy. This explains the fact that the excited beryllium ions, whose decay results in the emission of lines λ313.0 nm, get considerable kinetic energy.

CONCLUSION

In the paper the annealing effect on the secondary particle emission at ion bombardment of zirconium alloy (volumetric metallic glass) $Zr_{41}Ti_{11}Cu_{12.5}Ni_{10}Be_{22.5}$ was studied. X-ray diffraction analysis showed that the structure of the initial samples, that had not been annealed, was amorphous. Annealing for 1 hour at 773 K leads to the formation of crystalline structure.

The dose dependency of low-energy secondary ions analyzed with SIMS method showed the presence of three types of ions: ions knocked out of the chemical compounds on the target surface under the influence of the gas phase; ions knocked out of the chemical compounds, which are formed on the surface due to desorption of the gas particles from the target volume, and cluster ions knocked out of the target volume. Similar dose dependences of the secondary ions caused by the desorption of hydrogen and oxygen indicate a weak desorption of gases from the investigated alloy in the temperature range up to 773 K.

Study of the spatial distribution of excited particle radiation carried out by the IPS method showed that the atoms and ions of the elements forming the investigated alloys, are mainly knocked out of the target volume. The velocity set of the knocked out excited particles depends on the crystalline state of the target. For the amorphous targets the probability collision cascade in the target volume is improbable.

Analysis of the influence of the nonradiative loss process of excitation (resonant ionization) on the velocity set of the excited particles knocked out under ion bombardment of the mentioned alloys showed that the value of the work function of these alloys is in the range of $3.93 < \varphi < 4.131$ eV.

REFERENCES

1. P. Murali, U. Ramamurty. Embrittlement of a bulk metallic glass due to sub-T_g annealing // *Acta Materialia*. 2005, v. 53, p. 1467-1478.

2. N.V. Pleshivtsev, A.I. Bazhin. *Fizika vozdeistviya ionnykh puchkov na materially*. M.: "Vuzovskaya kniga". 1998, 392 p. (in Russian).

3. M. Ait El Fgih. Ion-induced atomic excitation in aluminum and copper // *Armenian Journal of Physics*. 2010, v. 3, p. 292-296.

4. I.O. Afanas'eva, V.V. Bobkov, S.P. Gokov, et al. Effect of phase on the formation of excited particles under ion bombardment of Fe-Co alloys // V*acuum*. 2010, v. 84, p. 1011-1013.

5. V.V. Bobkov, I.A. Afanas'eva, V.V. Gritsyna, et al. Characteristic features of ion-photon emission from

yttrium-iron garnets // *Vacuum.* 2012, N 86, p. 1624-1629.

6. V.V. Gritsyna, A.G. Koval', V.T. Koppe i dr. Issledovanie izlucheniya vozbushdennykh chastits, otletayuschikh ot poverkhnosti mednoi misheni pri ionnoi bombardirovke // *Optika i spektroskopiya*. 1995, v. 78, p. 212-216 (in Russian).

7. G.E. Abrosimova, A.S. Aronin, D.V. Matveev, V.V. Molokanov. Formation and structure of nanocrystals in bulk $Zr_{50}Ti_{16}Cu_{15}Ni_{19}$ metallic glass // *Physics of the Solid State*. 2004, v. 46, p. 2119-2123.

8. M. Ait El Fqih, P.G. Fournier. Ion beam sputtering monitored by optical spectroscopy // *Acta Physica Polonica A.* 2009, v. 115, p. 849-853.

9. V.M. Azhazha, A.M. Bovda, A.E. Dmitrenko i dr. Issledovanie protsessov sorbtsiidesorbtsii vodoroda iz bystrozakalyonnykh splavov sistemy Ti-Zr-Ni // *Probl. of Atomic Science and Tecnology*. 2006, №15, p. 156-161 (in Russian).

10. S.F. Belykh, A.B. Tolstoguzov, A.A. Lozovan, et al. Model for the emission of quasithermal atoms during sputtering of metals in the nonlinear collision cascade regime // *Journal of Experimental and Theoretical Physics*. 2014, v. 118, p. 560-568.

11. V.V. Bobkov, S.P. Gokov V.V. Gritsyna, D.I. Shevchenko, S.S. Alimov. Mechanism of formation of sputtered particles in excited states at Ar^+ ion bombardment on the oxide targets // *Nucl. Instrum. Meth.* 2007, v. B256, p. 501-505.

12. R. Behrisch. *Sputtering by particle bombardment I.* Berlin-Heidelberg-New-York: "Springer-Verlag", 1981, 278 p.

13. V.A. Pozdzersky, B.A. Tsipinyuk. Excited atom emission from metals under ion bombardment // *Vacuum*. 1982, v. 32, p. 723-728.

14. K. Luo, W. Li, H.Y. Zhang, H.L. Su. Changes of hardness and electronic work function of $Zr_{41.2}Ti1_{3.6}Cu_{12.5}Ni_{10}Be_{22.5}$ bulk metallic glass on annealing // *Philosopical Magazin Letter*. 2011, v. 91, p. 267-245.

15. V.E. Yurasova, L.F. Urazgildin. Charge exchange features of excited sputtered particle production // *Rad. Eff. and Def. in Sol*. 1991, v. 117, p. 99-111.

16. V.V. Gritsyna, A.G. Koval', S.P. Gokov, D.I. Shevchenko. Ion-photon emission of titanium-containing targets and its use for analysis of the composition of the surface // *Ukr. Fiz. Zh*. 2000, v. 45, p. 265-269.

Article received 06.07.2017

ВЛИЯНИЕ ОТЖИГА НА ЭМИССИЮ ВТОРИЧНЫХ ЧАСТИЦ С ПОВЕРХНОСТИ ЦИРКОНИЕВОГО СПЛАВА

И.А. Афанасьева, В.В. Бобков, В.В. Грицына, К.В. Ковтун, В.Т. Коппе, В.А. Литвинов, И.И. Оксенюк, С.В. Ховрич, Д.И. Шевченко

Эмиссия вторичных ионов и возбужденных частиц при ионной бомбардировке исследована методами вторичной ионной масс-спектрометрии (ВИМС) и ионно-фотонной спектрометрии (ИФС). Установлено, что зависимость выхода вторичных частиц от дозы облучения (вплоть до $3{,}5\cdot10^{17}$ ион·см$^{-2}$) имеет различный вид для частиц, выбитых из химических соединений на поверхности и из объема мишени. Показано, что пространственное распределение излучения вторичных возбужденных частиц отличается для аморфного и кристаллического стекол. Из анализа влияния процесса резонансной ионизации на вероятность отлета частиц в возбужденном состоянии сделана оценка значения работы выхода объемного аморфного стекла $Zr_{41}Ti_{14}Cu_{12,5}Ni_{10}Be_{22,5}$ ($3{,}93 < \varphi < 4{,}131$ эВ).

ВПЛИВ ВІДПАЛУ НА ЕМІСІЮ ВТОРИННИХ ЧАСТИНОК З ПОВЕРХНІ ЦИРКОНІЄВОГО СПЛАВУ

І.О. Афанасьєва, В.В. Бобков, В.В. Грицина, К.В. Ковтун, В.Т. Коппе, В.О. Літвінов, І.І. Оксенюк, С.В. Ховрич, Д.І. Шевченко

Емісія вторинних іонів та збуджених частинок при іонному бомбардуванні досліджена методами вторинної іонної мас-спектрометрії (ВІМС) та іонно-фотонної спектрометрії (ІФС). Встановлено, що залежність виходу вторинних частинок від дози опромінення (до $3{,}5\cdot10^{17}$ іон·см$^{-2}$) має різний вигляд для частинок, вибитих з хімічних сполук на поверхні та з об'єму мішені. Показано, що просторовий розподіл випромінювання вторинних збуджених частинок відрізняється для аморфного і кристалічного скла. З аналізу впливу процесу резонансної іонізації на ймовірність відльоту частинок у збудженому стані зроблена оцінка значення роботи виходу об'ємного аморфного скла $Zr_{41}Ti_{14}Cu_{12,5}Ni_{10}Be_{22,5}$ ($3{,}93 < \varphi < 4{,}131$ еВ).